

A study of elliptic flows in a quark combination model

Tao Yao,¹ Qu-bing Xie,¹ and Feng-lan Shao²

¹*Department of Physics, Shandong University, Jinan, Shandong 250100, P. R. China*

²*Department of Physics, Qufu Normal University, Qufu, Shandong 273165, P. R. China*

We carry out a detail study of elliptic flows in Au-Au collisions at 200 AGeV in a quark combination model. We find that elliptic flow data for a variety of hadrons can be well reproduced except pions if constituent quarks with equal parallel transverse momenta combine into initially produced hadrons. In a combination mechanism where initial hadrons are formed by quarks with unequal parallel transverse momenta, theoretical predictions agree with data for all available hadrons including pions. The mass hierarchy at low transverse momenta in elliptic flows can be understood in the same quark combination mechanism as in the mediate range of transverse momenta.

PACS number: 25.75.-q, 25.75.Ld, 12.40.-y

Keywords: Heavy ion collision, collective flow, quark matter, quark combination model, the mass hierarchy of elliptic flows

I. INTRODUCTION

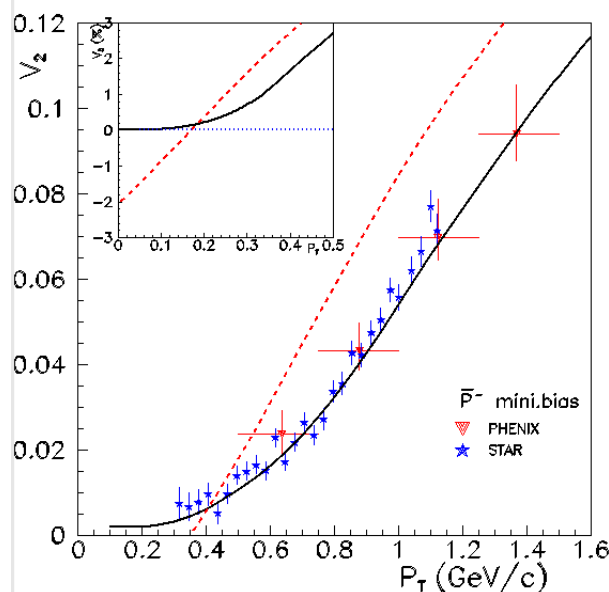
The elliptic flow is one of the most important observables in ultra-relativistic heavy ion collisions, which carries a lot of information about the initial state of the dense matter [1, 2, 3, 4]. The elliptic flow v_2 for a hadron is defined as the coefficient of the term $\cos 2\phi$ in the Fourier expansion of the invariant differential cross section $E \frac{d^3N}{d^3P}$, where ϕ is the azimuthal angle of the hadron momentum in the transverse plane [5, 6]. The E877 collaboration first measured the anisotropic flow in heavy ion collisions at AGS energies. In recent years, a thorough experimental study of elliptic flows for various hadrons has been taken at relativistic heavy ion collider (RHIC) energies. The elliptic flows as functions of centrality, pseudorapidity and transverse momentum have been measured. Various theoretical models have been proposed to describe data, such as coalescence or recombination models [7, 8, 9, 10], transport models [11, 12, 13], and hydrodynamic models [14, 15, 16] etc..

A salient feature of $v_2(p_T)$ at mediate transverse momenta p_T is the quark number scaling, i.e. when both v_2 and p_T rescaled by the constituent quark number n_q of the hadron, the elliptic flow is a universal function of p_T for all hadrons. The quark number scaling of the elliptic flow and the abnormal ratio of baryons to mesons at mediate p_T support the quark recombination mechanism in hadron formation. However, at small transverse momenta p_T the quark number scaling is not obvious, instead, there is a different structure the so-called mass hierarchy [17] in data. In hydrodynamic models, the mass hierarchy arises from radial flows which are hadron masses [15] dependent. But hydrodynamic models cannot describe elliptic flow data at mediate and high p_T . The mass hierarchy structure of $v_2(p_T)$ for charged pions and kaons and protons/anti-protons has been reproduced by a multi-phase transport model [18]. In the large p_T range of about 10 GeV/c, Ref. [19, 20, 21] have described the global behavior of $v_2(p_T)$ for some hadrons in combination mechanism, but the mass hierarchy of $v_2(p_T)$ for various hadrons at low p_T has not been fully compared with experiment data or reproduced within coalescence/recombination models. Ref. [22, 23] and some models have given several possible origins of the mass hierarchy, however, we show decay is one of the most important reasons and give another explanation for the mass hierarchy. In this paper, we carry out a detail study of elliptic flows in a quark combination model in the whole p_T range with a special focus on the mass hierarchy or fine structure at low p_T . We will show that the fine structure of elliptic flows can be well described in the quark combination picture provided initially produced hadrons and resonance decays are treated separately and properly.

II. QUARK COMBINATION MODEL

All kinds of hadronization models demand themselves, consciously or not, satisfy rapidity or momentum correlation for quarks in the neighborhood of phase space. The essence of this correlation is its agreement with the fundamental requirement of QCD which uniquely determines the quark combination rule [24, 25]. According to QCD, a $q\bar{q}$ may be in a color octet or a singlet which means a repulsive or an attractive interaction between them. The smaller the difference in rapidity for two quarks is, the longer the interaction time is. So there is enough time for a $q\bar{q}$ to be in a color singlet and form a meson. Similarly, a qq can be in a sextet or an anti-triplet. If its nearest neighbor is a q in rapidity, they form a baryon. If the neighbor is a \bar{q} , because the attraction strength of the singlet is two times that of the anti-triplet, $q\bar{q}$ will win the competition to form a meson and leave a q alone.

Figure 1: The $v_2(p_T)$ spectra for final state anti-proton from Eq. (1) (dashed line) and (2) (solid line). The sub-diagram in the upper-left corner shows curves of Eq. (1) (dashed line) and (2) (solid line).

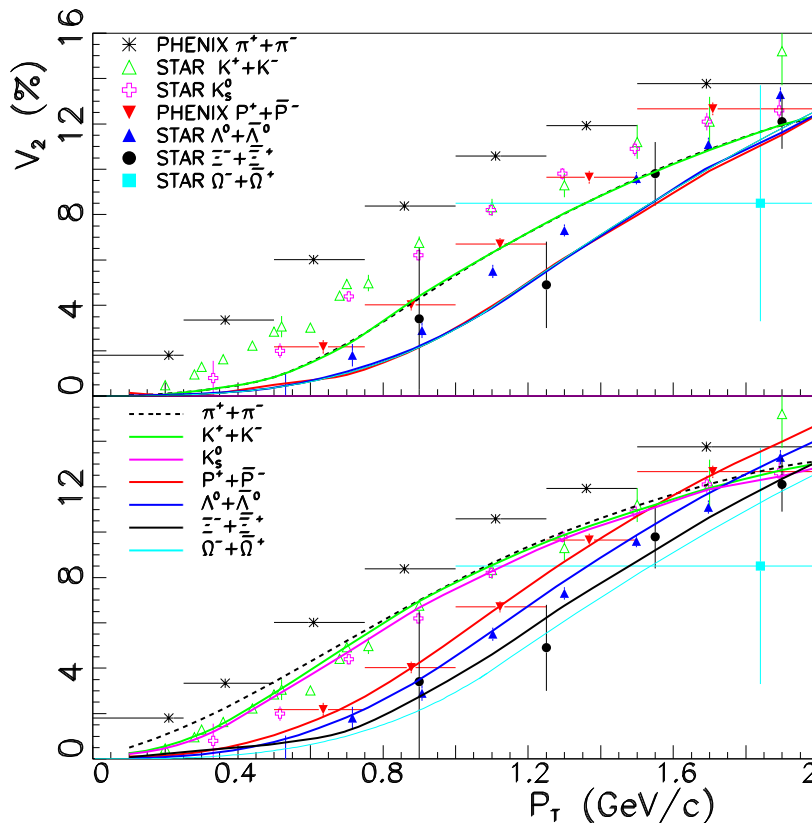


We have developed a variant of the quark combination model (QCM) based on a simple quark combination rule [24, 25] incorporating the above QCD requirements. The flavor $SU(3)$ symmetry with strangeness suppression in the yields of initially produced hadrons is fulfilled in our QCM [24, 26]. Using our QCM, we have described most of multiplicity data for hadrons in electron-positron and proton-proton/anti-proton collisions [24, 26, 27, 28, 29, 30]. Also we solved a difficulty facing other QCMs in describing the TASSO data for baryon-antibaryon correlation in electron-positron collisions: they can be successfully explained by our QCM [25, 30]. Our QCM can also combine with the color flow picture [31] to describe the hadronization of multiparton states [32, 33, 34]. We have extended our QCM to reproduce the recent RHIC data for hadron multiplicities and p_T spectra [35].

In this paper we present a detail analysis of $v_2(p_T)$ in the whole p_T range based on our QCM. We put particular emphasis on the low p_T region where the elliptic flow data for various hadrons show non-trivial fine structure. Our treatment of elliptic flows is different from other coalescence or recombination models [19, 20]. We extract $v_{2,q}(p_T)$ for quarks as input from fitting the experiment data of various hadrons. So we can construct elliptic flows for all initially produced hadrons from $v_{2,q}(p_T)$ for quarks in our QCM. Then we let all resonances decay by using the decay program of the event generator PYTHIA [36] to obtain elliptic flows for final state hadrons. One advantage of using PYTHIA to deal with decays is that all available decay channels are covered. Here we only take into account light quarks in hadronization. In central Au-Au collisions at 200 AGeV, the yield of charm hadrons is about 28 in the whole rapidity range [37]. So charm quarks are negligible compared to light quarks in $v_2(p_T)$ for final state hadrons.

III. RESULTS AND ANALYSIS

In order to describe data of elliptic flows, only those quarks with collinear momenta are allowed to combine into hadrons, because the combination of constituent quarks in different momentum directions would lead to large invariant masses which are off-mass-shell for most hadrons. To describe data in central rapidity, we choose the rapidity range $y \in [-0.5, 0.5]$ for hadrons in our calculation. We also assume that quarks and antiquarks of a same flavor have the same $v_{2,q}(p_T)$. Considering that the coalescence or recombination models work very well at mediate p_T , we focus our study on elliptic flows at low p_T which have not been well investigated in combination-like models. We assume three collinear combination strategies, the naive scheme with equal p_T combination and the same $v_{2,q}(p_T)$ for quarks of all flavors, the modified naive scheme with equal p_T combination and a different $v_{2,q}(p_T)$ for strange quarks from light quarks, and the scheme with different p_T combination.

Figure 2: The $v_2(p_T)$ spectra for directly produced (upper panel) and final state (lower panel) hadrons from Eq. (2).

A. Naive combination scheme

In this scheme, all u , d and s quarks are assumed to have the same $v_{2q}(p_T)$ spectrum. The quarks with equal p_T combine into hadrons. Our input is based on

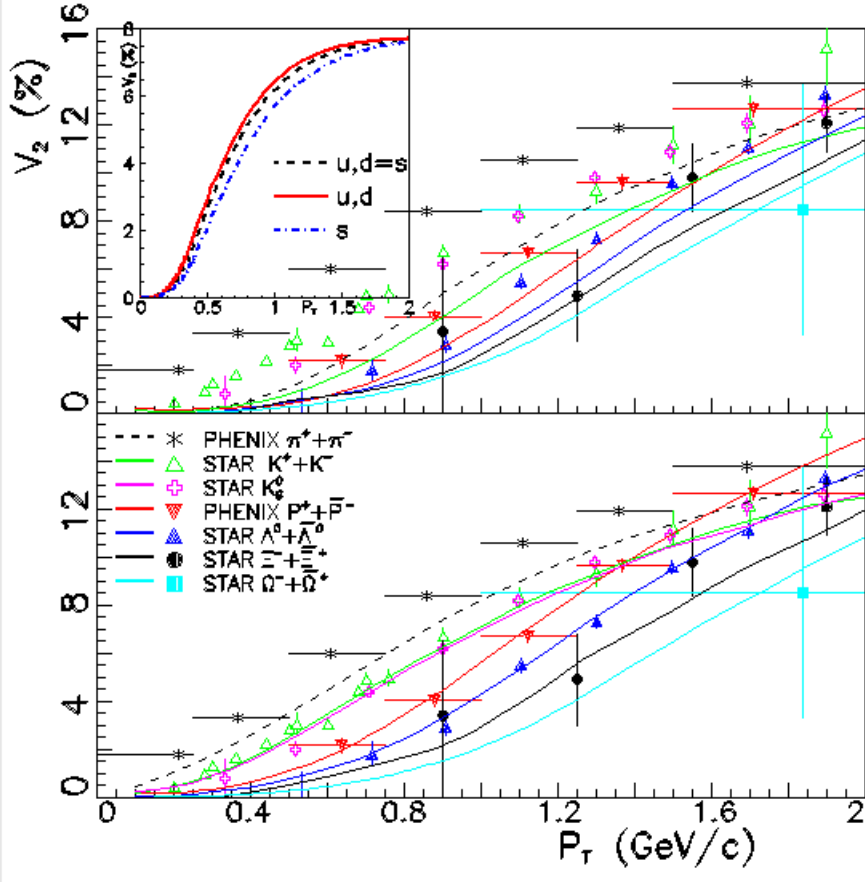
$$v_{2q}^{(0)}(p_T) = 0.078 \tanh(1.59p_T - 0.27) \quad (1)$$

for quarks given in Ref. [38] by fitting the proton data. Hereafter the unit of p_T is GeV. We make two improvements, one is that the decay contributions have been subtracted, the other is that the negative part of $v_{2q}^{(0)}(p_T)$ inconsistent to data and to the expected quadratic behavior [22, 39] at small p_T (see the dashed line in Fig. 1) is corrected to be positive. The improved $v_{2,q}(p_T)$ is given by

$$\begin{aligned} v_{2,q}(p_T) &= 0.256p_T^3, & 0 \leq p_T \leq 0.365, \\ v_{2,q}(p_T) &= 0.078 \tanh[1.45(p_T - 0.25)], & p_T > 0.365. \end{aligned} \quad (2)$$

Note that considering the continuity of the Eq. (2), we adopt the p_T^3 instead of the p_T^2 form. The difference resulted from the two function forms at low p_T range can be neglected for the coefficient of p_T^3 or p_T^2 is adjustable. One sees that the data for antiprotons are well reproduced at small p_T with the above input, see the solid line in Fig. 1. Moreover it can fit all hadron data except pions as shown in the lower panel of Fig. 2. Note that in figures following Fig. 2 the order of curves from left to right is the same that of data for various hadrons. The STAR data in Fig. 1 are taken from Ref. [17]. In Fig. 1 and 2, the PHENIX data are taken from Ref. [40]. In Fig. 2, the data for K_S^0 and $\Lambda + \bar{\Lambda}$ are from Ref. [41], the data for $\Xi^- + \bar{\Xi}^+$ and $\Omega^- + \bar{\Omega}^+$ are from Ref. [42], and the data for kaons are from Ref. [17].

In the naive combination scheme, directly produced mesons and baryons have the same elliptic flows $v_{2,M}(p_T) = 2v_{2,q}(p_T/2)$ and $v_{2,B}(p_T) = 3v_{2,q}(p_T/3)$ respectively, regardless of their masses and species. Comparing the upper and

Figure 3: The $v_2(p_T)$ spectra for directly produced (upper panel) and final state (lower panel) hadrons from Eq. (3).

lower panels of Fig. 2, one observes that the $v_2(p_T)$ curve for the hadron i shifts somewhere in the left depending on how much the decay contributions the hadron has. One sees that the fine structure of $v_2(p_T)$ for hadrons at small p_T results from decay contributions. But for pions it is not enough to reproduce the data by only including the decays, one has to take into account other effects. We will address this issue in the modified naive combination scheme in the next subsection.

B. Modified naive combination scheme

In this scheme, we take into account that $v_{2,q}(p_T)$ for strange quarks is different from light quarks. The difference is mainly at small p_T since the quark mass effects barely influence the magnitude of $v_2(p_T)$ at mediate p_T , see the attached figure in the upper-left corner in the upper panel of Fig. 3. Note that Ref. [19, 20] also include the strange-light difference. We know that the strongly coupled quark-gluon-plasma produced at RHIC is relativistic fluid, then we can assume that the average transverse momenta for u , d and s quarks are proportional to their average energies, $\frac{\langle p_T \rangle_{u,d}}{\langle p_T \rangle_s} \approx \frac{\langle E \rangle_{u,d}}{\langle E \rangle_s}$. Based on this relation, we modify $v_{2,q}(p_T)$ for u , d and s quarks as,

$$\begin{aligned} v_{2,i}(p_T) &= 0.256(p_T/\alpha_i)^3, \quad 0 \leq p_T/\alpha_i \leq 0.365, \\ v_{2,i}(p_T) &= 0.078 \tanh[1.45(p_T/\alpha_i - 0.25)], \quad p_T/\alpha_i > 0.365. \end{aligned} \quad (3)$$

where $i = u, d, s$ and α_i is given by

$$\begin{aligned} \alpha_{u,d} &= \frac{2 \langle E \rangle_{u,d}}{\langle E \rangle_{u,d} + \langle E \rangle_s} \approx 0.94, \\ \alpha_s &= \frac{2 \langle E \rangle_s}{\langle E \rangle_{u,d} + \langle E \rangle_s} \approx 1.12. \end{aligned} \quad (4)$$

Figure 4: The $v_2(p_T)$ spectra for final state hadrons are given in the upper panel. The $v_2(p_T)$ spectra scaled by constituent quark number are given in the lower panel. The theoretical curves are results in the unequal momentum combination scheme.

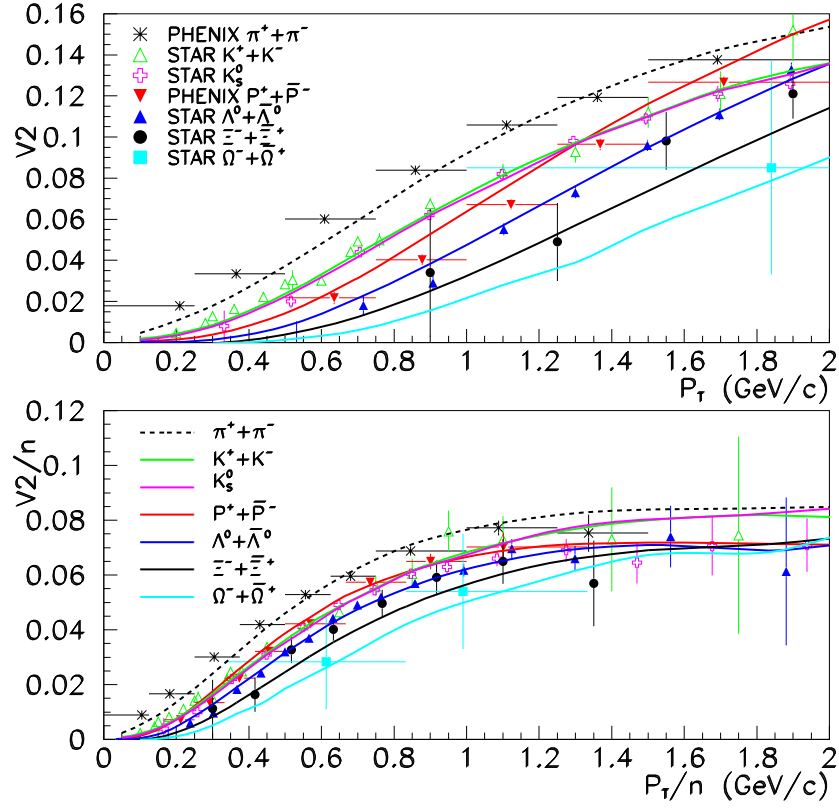
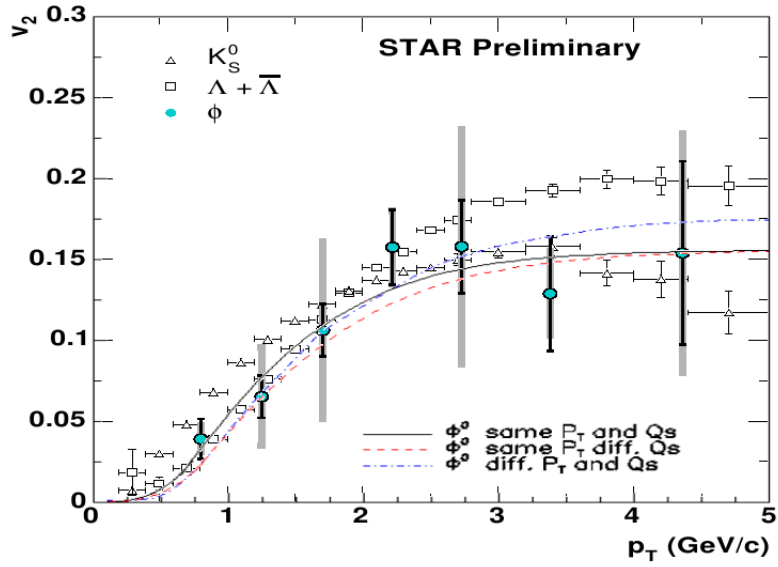


Figure 5: The $v_2(p_T)$ spectra for ϕ mesons in three combination schemes.



where the average values of quark energies can be approximated as $\langle E \rangle_f \approx \sqrt{m_f^2 + \langle p_T^2 \rangle}$ with constituent quark mass m_f for the flavor f ($m_{u,d} = 0.34$ GeV, $m_s = 0.5$ GeV) and with $\langle p_T^2 \rangle$ given by the distribution $f(p_T) = (p_T^{2.3} + p_T^{0.2} + 1)^{-3.0}$ from Ref. [35]. Here we have implied the central rapidity $y \approx 0$ in estimating the average energy. Based on the input for quark elliptic flows in Eq. (3), $v_2(p_T)$ for meson and baryon are written as

$$\begin{aligned} v_{2,M}(p_T) &\approx v_{2,i}(p_T/2) + v_{2,j}(p_T/2), \\ v_{2,B}(p_T) &\approx v_{2,i}(p_T/3) + v_{2,j}(p_T/3) + v_{2,k}(p_T/3), \end{aligned} \quad (5)$$

with i, j denote the constituent quarks in the meson M and i, j, k denote those in the baryon B . Therefore the $v_2(p_T)$ curves for hadrons with the same flavor content are identical. The results in this combination scheme are shown in Fig. 3. In contrast to Fig. 2, the $v_2(p_T)$ curves for directly produced hadrons split according to their flavor contents and lead to even larger splittings for final state hadrons. The pion curve is partially improved but not enough to match the data. For other hadrons, the agreement between theoretical predictions and data is satisfactory. Although tuning $\alpha_{u,d}$ to a smaller value would make pion curve fit the data, the fine structure of $v_2(p_T)$ for other hadrons prevent them from splitting too much. The results show that in the quark combination mechanism the quark mass effect and resonance decays partially account for the fine structure of $v_2(p_T)$ for final state hadrons. In contrast to the hydro-model interpretation of differences among hadron $v_2(p_T)$ as hadron mass effects, the mass effects at the quark level is partially responsible for such differences in the quark combination picture. To identify the mass effects of strange quarks and light quarks, a better way is to measure and compare $v_2(p_T)$ for ϕ and K^* in experiments.

C. Unequal p_T combination scheme

As shown in Fig. 3, it is still not enough to reproduce the pion data by including resonance decays and the quark mass effect. In order to better fit the pion data together with all other hadrons, we relax in this scheme the constraint that quarks with equal p_T combine into hadrons by allowing unequal p_T combination. The unequal p_T combination is more general than the equal one which can be regarded as a special case of the former. Since the combination condition is changed, we then start with a different form of $v_{2,q}(p_T)$ for quarks from that in the equal p_T combination schemes,

$$v_{2,q}(p_T) = 0.286p_T^4, \quad 0 \leq p_T \leq 0.525, \quad (6)$$

$$v_{2,q}(p_T) = 0.11 \tanh[1.6(p_T - 0.4)], \quad p_T > 0.525. \quad (7)$$

The results for hadron $v_2(p_T)$ are shown in Fig. 4. The initial hadrons with the same flavor contents have an identical curve. One sees in the upper panel that the pion curve agrees with data very well. Note that Ref. [38] reproduces the pion data after taking into account the momentum distribution of hadrons, a similar strategy to ours, and Ref. [43] takes into account the resonance decay contribution to pions. In contrast, we give the results for other hadrons also fit the data besides pions. The main difference from the equal p_T combination scheme is that $v_2(p_T)$ spectra for hadrons at mediate p_T split into two groups (of mesons and baryons), i.e. there is no exact quark number scaling, but theoretical predictions are still within the error bars. More precise measurements are needed to distinguish the two combination schemes in the mediate p_T range. Obviously the fine structure of $v_2(p_T)$ at low p_T is a joint effect of resonance decays, the quark mass difference in $v_{2,q}(p_T)$ and unequal p_T combination. The reason that the unequal p_T combination works well at low and mediate p_T lies in the fact that it splits the spectra for different hadrons at the cost of slightly spoiling the quark number scaling. But the data are not sensitive to such a violation of the scaling.

In Fig. 5, we give the predictions for ϕ mesons in three combination schemes. The agreement with recent STAR data is satisfactory [44]. In all of our calculations, we neglect the influence of hadron re-scattering on $v_2(p_T)$, same as in Ref. [38].

IV. SUMMARY

We use quark combination model to study elliptic flows for directly produced hadrons before resonant decays and the final state hadrons. Especially we have investigated the fine structure of elliptic flows at small p_T . We find the combination mechanism works very well in describing elliptic flow data in low p_T as well as in mediate p_T regime. In the scheme with equal p_T combination and equal input function for $v_{2,q}(p_T)$ for light and strange quarks, the data for all hadrons can be well reproduced except pions, where the fine structure can be understood by the decay contributions. Taking into account the mass effect of the input function $v_{2,q}(p_T)$ for light and strange quarks and assuming unequal p_T combination, the overall agreement between our predictions and all available data for hadrons

including pions are satisfactory. The decay contributions and the mass effect of the input function $v_{2,q}(p_T)$ for quarks play important roles. The directly produced hadrons with the same flavor content have an identical $v_2(p_T)$ spectrum, which is an obvious feature of the quark combination mechanism.

Acknowledgments

The authors thank Shi-yuan Li, Zuo-tang Liang, Zong-guo Si for helpful discussions. Special thanks go to Qun Wang for critically reading the manuscript with many suggestions. The work is supported in part by National Natural Science Foundation of China (NSFC) under grant 10475049.

-
- [1] J. Y. Ollitrault, Phys. Rev. D **46**, 229 (1992).
[2] H. Sorge, Phys. Rev. Lett. **82**, 2048 (1999) [arXiv:nucl-th/9812057].
[3] J. Barrette *et al.* [E877 Collaboration], Phys. Rev. Lett. **73**, 2532 (1994) [arXiv:hep-ex/9405003].
[4] H. Appelshauser *et al.* [NA49 Collaboration], Phys. Rev. Lett. **80**, 4136 (1998) [arXiv:nucl-ex/9711001].
[5] S. Voloshin and Y. Zhang, Z. Phys. C **70**, 665 (1996) [arXiv:hep-ph/9407282].
[6] A. M. Poskanzer and S. A. Voloshin, Phys. Rev. C **58**, 1671 (1998) [arXiv:nucl-ex/9805001].
[7] D. Molnar and S. A. Voloshin, Phys. Rev. Lett. **91**, 092301 (2003) [arXiv:nucl-th/0302014].
[8] R. C. Hwa and C. B. Yang, Phys. Rev. C **67**, 034902 (2003) [arXiv:nucl-th/0211010].
[9] R. J. Fries, B. Muller, C. Nonaka and S. A. Bass, Phys. Rev. Lett. **90**, 202303 (2003) [arXiv:nucl-th/0301087].
[10] V. Greco, C. M. Ko and P. Levai, Phys. Rev. Lett. **90**, 202302 (2003) [arXiv:nucl-th/0301093].
[11] M. Bleicher and H. Stoecker, Phys. Lett. B **526**, 309 (2002) [arXiv:hep-ph/0006147].
[12] Z. w. Lin and C. M. Ko, Phys. Rev. C **65**, 034904 (2002) [arXiv:nucl-th/0108039].
[13] D. Teaney, J. Lauret and E. V. Shuryak, Nucl. Phys. A **698**, 479 (2002) [arXiv:nucl-th/0104041].
[14] P. F. Kolb, J. Sollfrank and U. W. Heinz, Phys. Rev. C **62**, 054909 (2000) [arXiv:hep-ph/0006129].
[15] P. Huovinen, P. F. Kolb, U. W. Heinz, P. V. Ruuskanen and S. A. Voloshin, Phys. Lett. B **503**, 58 (2001) [arXiv:hep-ph/0101136].
[16] N. Borghini and J. Y. Ollitrault, arXiv:nucl-th/0506045.
[17] J. Adams *et al.* [STAR Collaboration], Phys. Rev. C **72**, 014904 (2005) [arXiv:nucl-ex/0409033].
[18] Z. w. Lin, C. M. Ko, B. A. Li, B. Zhang and S. Pal, Phys. Rev. C **72**, 064901 (2005) [arXiv:nucl-th/0411110].
[19] C. Nonaka, R. J. Fries and S. A. Bass, Phys. Lett. B **583**, 73 (2004) [arXiv:nucl-th/0308051].
[20] V. Greco, C. M. Ko and P. Levai, Phys. Rev. C **68**, 034904 (2003) [arXiv:nucl-th/0305024].
[21] R. J. Fries, B. Muller, C. Nonaka and S. A. Bass, Phys. Rev. C **68**, 044902 (2003) [arXiv:nucl-th/0306027].
[22] D. Molnar, arXiv:nucl-th/0408044.
[23] S. Pratt and S. Pal, Nucl. Phys. A **749**, 268 (2005) [Phys. Rev. C **71**, 014905 (2005)] [arXiv:nucl-th/0409038].
[24] Q. B. Xie and X. M. Liu, Phys. Rev. D **38**, 2169 (1988).
[25] Q. B. Xie, *Prepared for 19th International Symposium on Multiparticle Dynamics: New Data and Theoretical Trends, Arles, France, 13-17 Jun 1988*
[26] Q. Wang and Q. B. Xie, J. Phys. G **21**, 897 (1995).
[27] Z. . Liang and Q. . Xie, Phys. Rev. D **43**, 751 (1991).
[28] J. Q. Zhao, Q. Wang and Q. B. Xie, Sci. Sin. A **38**, 1474 (1995).
[29] Q. Wang, Z. G. Si and Q. B. Xie, Int. J. Mod. Phys. A **11**, 5203 (1996).
[30] Z. G. Si, Q. B. Xie and Q. Wang, Commun. Theor. Phys. **28**, 85 (1997).
[31] Q. Wang, Q. B. Xie and Z. G. Si, Phys. Lett. B **388**, 346 (1996).
[32] Q. Wang and Q. B. Xie, Phys. Rev. D **52**, 1469 (1995).
[33] Q. Wang, G. Gustafson and Q. b. Xie, Phys. Rev. D **62**, 054004 (2000) [arXiv:hep-ph/9912310].
[34] Q. Wang, G. Gustafson, Y. Jin and Q. b. Xie, Phys. Rev. D **64**, 012006 (2001) [arXiv:hep-ph/0011362].
[35] F. I. Shao, Q. b. Xie and Q. Wang, Phys. Rev. C **71**, 044903 (2005) [arXiv:nucl-th/0409018].
[36] T. Sjostrand, L. Lonnblad, S. Mrenna and P. Skands, arXiv:hep-ph/0308153.
[37] S. S. Adler *et al.* [PHENIX Collaboration], Phys. Rev. Lett. **94**, 082301 (2005) [arXiv:nucl-ex/0409028].
[38] V. Greco and C. M. Ko, Phys. Rev. C **70**, 024901 (2004) [arXiv:nucl-th/0402020].
[39] P. Danielewicz, Phys. Rev. C **51**, 716 (1995) [arXiv:nucl-th/9408018].
[40] S. S. Adler *et al.* [PHENIX Collaboration], Phys. Rev. Lett. **91**, 182301 (2003) [arXiv:nucl-ex/0305013].
[41] J. Adams *et al.* [STAR Collaboration], Phys. Rev. Lett. **92**, 052302 (2004) [arXiv:nucl-ex/0306007].
[42] J. Adams *et al.* [STAR Collaboration], Phys. Rev. Lett. **95**, 122301 (2005) [arXiv:nucl-ex/0504022].
[43] X. Dong, S. Esumi, P. Sorensen, N. Xu and Z. Xu, Phys. Lett. B **597**, 328 (2004) [arXiv:nucl-th/0403030].
[44] X. z. Cai [STAR Collaboration], arXiv:nucl-ex/0511004.